

Prediction of turn down warping during hot plate rolling based on a Gaussian function

Jae Hyung Seo¹ · Chester J. VanTyne² · Young Hoon Moon³

Received: 16 April 2015 / Accepted: 6 August 2015 / Published online: 19 August 2015
© Springer-Verlag France 2015

Abstract Turn down warping is a shape defect observed at the front end of a plate during hot rolling. To produce a flat plate without warping, a precise prediction of turn down warping is essential to achieve optimal control. Therefore, we propose a model based on a Gaussian function to predict turn down warping. The model uses the results from numerical analyses of hot plate rolling. The finite element code MARC was used for the numerical analysis. Hot plate rolling processing parameters, such as roll diameter, plate dimension, rolling speed, and pass line were all considered in the model. To verify the accuracy of the prediction model, the numerical results obtained by FEM were confirmed with data measured during industrial hot plate rolling. For the actual measurements of turn down warping, image processed high speed camera data from the exit side of the rolling were used. The results show that the proposed Gaussian function model can successfully predict turn down warping of a plate's front end under various hot plate rolling conditions.

Keywords Turn down · Warping · Hot rolling · Pass line · Gaussian function · Finite element analysis

Introduction

Turn down warping is a shape defect that occurs at the front end of a plate during hot rolling. Asymmetrical conditions during rolling can cause curvature and can lead to poor product shape and reduced productivity [1, 2].

Rolling under asymmetrical conditions may cause rolled plates to bend toward the direction of one of the rolls. Both turn-up and turn-down can cause problems with production, since damage to the rolls, the housing, and/or the run-out tables can all result. Production delays can also occur, due to stability issues when the plate is moved [3–8].

Figure 1 schematically shows the mechanism of turn down warping. The front end bending in Fig. 1a is based on the curvature $1/\rho_1$ of the rolled stock. The curvature of rolled stock shows the arc-of-a-circle-like bending. Figure 1b shows down bending and bending deflection during rolling. Figure 1c shows turn-down warping. In practice, the rolled stock warpage can be observed by the changes in its bending direction, as well as in its bending radius, (i.e. ρ_1 , ρ_2 , ρ_3 , etc.) over various distances.

It is important to prevent turn down warping during plate rolling. Once turn down warping happens, plate leveling is required to flatten the warped shape. Figure 2 shows the warped plate as it passes through pre-leveling, hot-leveling, cold leveling, and press levelling.

In order to achieve better dimensional control, it is necessary to achieve a greater understanding of the relationship between process parameters and turn down warping.

Studies of rolling curvature have been conducted through the use of experimental, analytical, and numerical techniques. M. Philipp et al. [9] have investigated front end bending from the viewpoints of speed mismatch and geometry. The bending curvature was found to correlate with a shape factor and the amount of reduction. Previous investigations [10–16] on turn

✉ Young Hoon Moon
yhmoon@pusan.ac.kr

¹ R&D Laboratory, POSCO, Pohang, Republic of Korea

² Department of Metallurgical and Materials Engineering, Colorado School of Mines, Golden, CO 80401, USA

³ School of Mechanical Engineering, Pusan National University, Busan 609-735, Republic of Korea

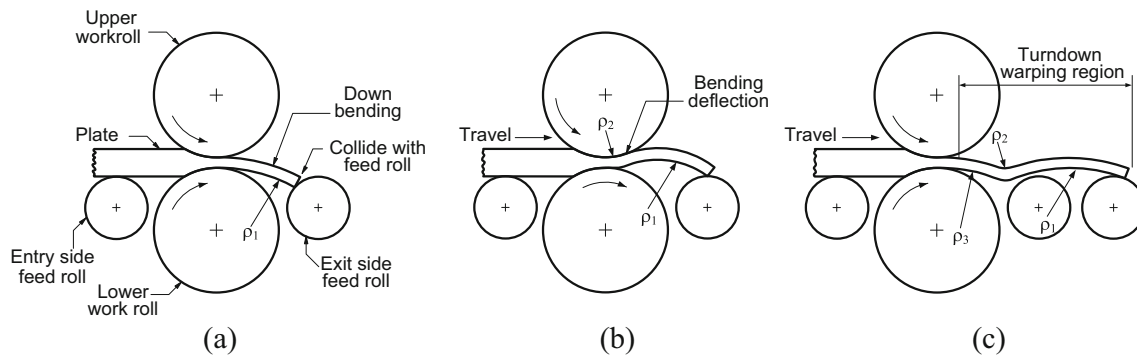


Fig. 1 Undesirable down bending and turn down warping in hot rolling of plate: **a** Front end bending; **b** Down bending and bending deflection; **c** Turn down warping

down warping concentrated on the effects of friction ratio, speed ratio, shape ratio, and reduction based on speed mismatch conditions. Unfortunately, the essential mechanisms and the sensitivity of the influencing parameters on asymmetric rolling are still not sufficiently understood. In many cases, the application of a controlled asymmetric process for plate rolling is advantageous to eliminate or minimize the effects of various factors that can influence process stability and the curvature of the front end of a rolled plate [17]. Severe plastic deformation can originate from asymmetries due to differences in size, rotational speed, and frictional conditions between upper and lower rolls. Such deformation can be an effective method for producing fine-grained materials [18–22]. As the speeds of the upper and lower work rolls are generally the same in production rolling, the prediction of turn down warping for conditions of matching speeds must be more intensively investigated.

The objectives of this paper are: 1) to predict turn down warping during hot plate rolling; 2) to obtain quantitative relationships between causes and effects of turn down warping; and 3) to suggest potential means of controlling turn down warping.

In the present investigation, a model based on a Gaussian function using the results of numerical analyses is proposed to predict turn down warping during hot plate rolling. A finite element method (FEM) was used for numerical analysis. Hot plate rolling process parameters, such as roll diameter, plate dimension, rolling speed and pass line, have all been considered. In the current study, the primary concern is warpage that occurs when roll speed match conditions are met. To verify the accuracy of the prediction model, numerical results of turn

down warping obtained by FEM were compared and confirmed with experimental data obtained from an operational line. For the actual measurement of turn down warping, image processing of high speed camera images taken on the exit side of the hot plate rolling was performed.

Analysis method

On-line measurement of turn down warping

As shown in Fig. 2, a shape image pattern was obtained by a high-speed camera at the second feed roll on the exit side. To analyze the shape pattern of turn down warping, numerous images were obtained during plate rolling. Image processing based on color contrast was used to quantitatively analyze these data. Figure 3 shows an example of the image pattern of turn down warping that was photographed during plate rolling.

Among the several shape patterns, the turn down warping pattern shown in Fig. 4 was considered in the current study.

Image data were obtained at the second exit feed roll of the finishing mill. From these images, the profile of turn down warping was obtained for a given length. The second exit feed roll of the finishing mill is used as a reference point for comparisons between measured and simulated warping.

Finite element simulation of turn down warping

Finite element simulations were performed to predict turn down warping with a speed match condition, using the

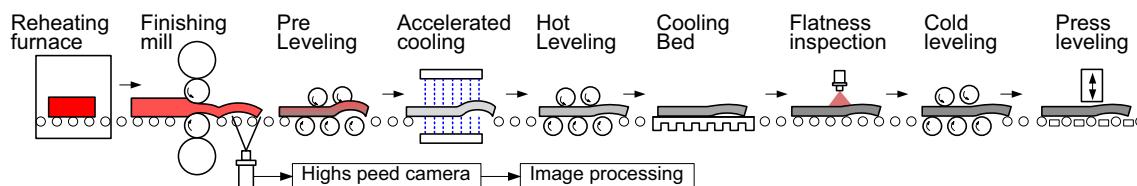


Fig. 2 Layout of plate making and leveling

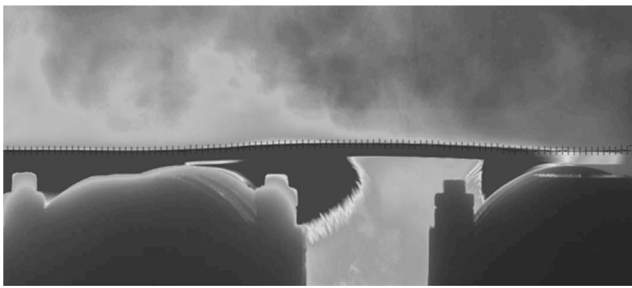


Fig. 3 Image pattern of turn down warping photographed during plate rolling (Seven frames were recorded per second)

commercial finite element software MSC.Marc/Mentat. Within the framework of this finite element model, the work roll and feed rolls were regarded as ideally rigid bodies rotating with equal and constant circumferential velocities. The plate was directed into the roll gap and the movement of the incoming plate was constrained in the vertical direction. The plate has an entry thickness of h_1 and is modeled as a deformable body with an elasto-plastic element type. For the sake of simplicity, the three-dimensional deformation phenomena (such as spreading of the processed material within the roll gap) are neglected, and a four-node, isoparametric, arbitrary quadrilateral written for plane strain applications has been used. As this element uses bilinear interpolation functions, the strains tend to be constant throughout the element. The initial temperature of the plate is set between 800 and 1000 °C, and the heat flow between the plate and the work rolls and the feed rolls was neglected. The flow curves used in the analysis is shown in Fig. 5.

Figure 6 shows the mesh used in the plate for the FE analysis. Ten sections were symmetrically modeled in the thickness direction, and the mesh heights at the contact surfaces of the upper and lower rolls were set to $\Delta_j/2$. For the plate travel direction, the mesh width of the front part of plate was set to be $\Delta_i/2$. The finer meshes enhance the stability of the simulation, especially at the entry stage of the plate entering the roll bite.

Figure 7 shows the layout for the FE model showing the plate, the work roll, and the feed roll, as well as other factors. The pass lines for simulation model were set to be 15, 25, 35, and 45 mm. The diameters of the upper work roll and the lower work roll are the same. For simplicity of the analysis, the upper and lower back-up rolls were not considered and the

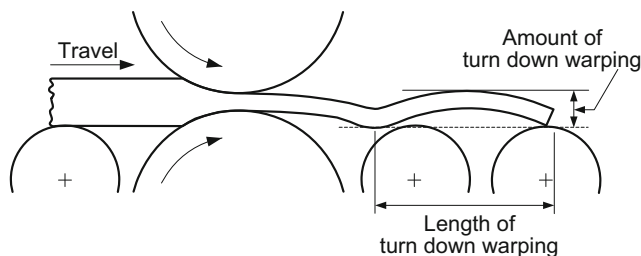


Fig. 4 Image pattern of turn down warping

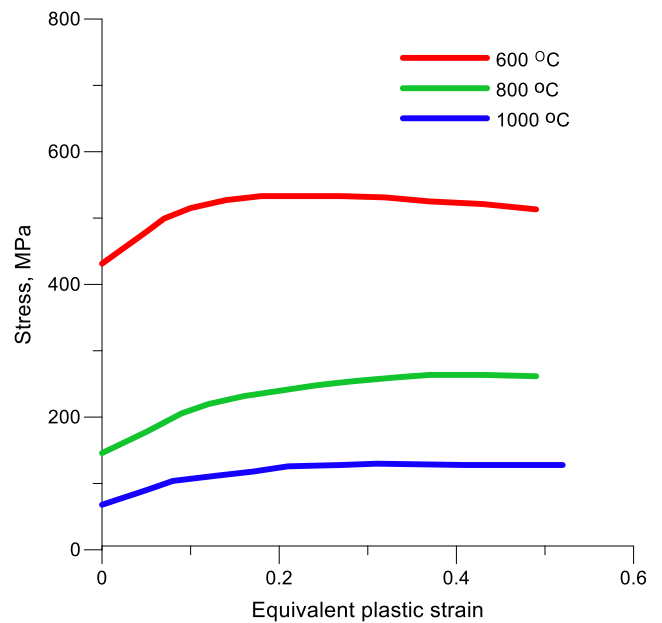


Fig. 5 High temperature flow curve of plate

tension at the front and back sides is ignored. As an external force, gravitational force has been considered and the processed material is assumed to be incompressible. For the speed match condition, the upper and lower work roll speeds are the same and resultant friction coefficients are also the same. The feed roll diameters at entry side and exit side are the same and roll speeds at entry side and exit side are also the same. Table 1 summarizes the FE simulation conditions.

The pass line, d , is the height difference between the work roll and feed roll. Mathematically,

$$d = \frac{(h_1 - h_2)}{2} + \delta \tag{1}$$

where, h_1 : entry thickness, h_2 : exit thickness, δ : constant to compensate work roll wear and thermal expansion. (Assumed zero in this study.) Fig. 8 schematically shows three cases of pass line.

The three cases shown in Fig. 8 assume a condition of speed matching, where the speed of both the upper and lower rolls is the same. Figure 8a shows the case where the pass line is equal to zero. As the contact angle, α_{upper} , forms only at the upper work roll, the upper side of the plate will be rolled and bending down will occur. In the case of symmetrical rolling, as shown in Fig. 8b, the same reduction at both sides of the plate prevents both bending up and/or bending down. When the contact angle, α_{lower} , forms only at the lower work roll as shown in Fig. 8c, the lower side of the plate will be rolled and bending up will occur. As expected, the situations shown in Fig. 8a and c are difficult to achieve in actual rolling, while the symmetrical rolling shown in Fig. 8b is most common. In symmetrical rolling, the pass line can cause turn down warping, and will be discussed below.

Fig. 6 Mesh formation of thickness direction and length direction

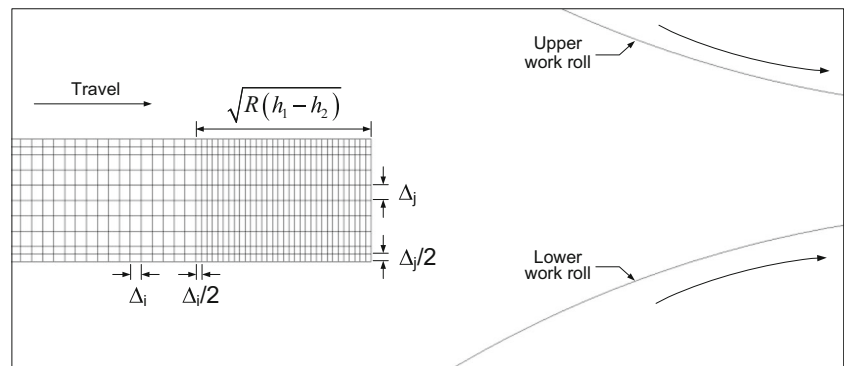
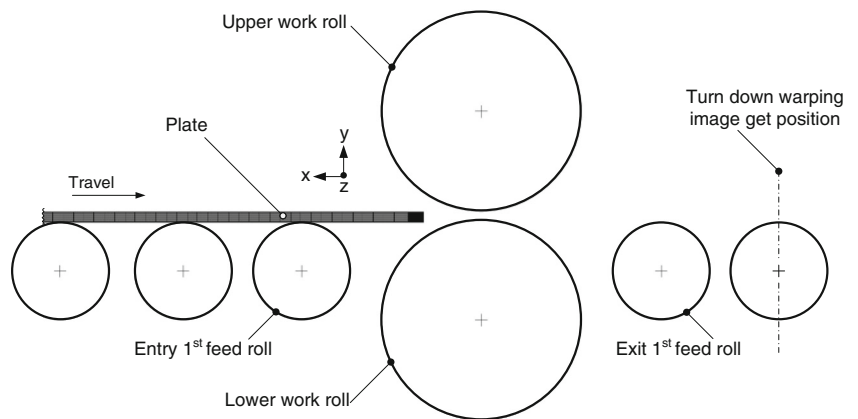


Fig. 7 The two-dimensional Finite Element Analysis model with work rolls and feed rolls



Results and discussion

Prediction model to predict turn down warping considering pass line

Results of the FE simulations have been used to understand which, among all of the rolling variables, are related to turn down warping. From the simulation results, regression analysis was performed to develop a model to predict turn down warping under a condition of speed matching.

Table 1 Simulation conditions for finite element analysis

Condition	Value
Plate material	C-Mn steel
Plate temperature	800 ~ 1000 °C
Work roll diameter ($d_{wr_{up}} = d_{wr_{low}}$)	1000 mm
Feed roll diameter ($d_{fr_{entry}} = d_{fr_{exit}}$)	500 mm
Friction coefficient ($\mu_{wr_{up}} = \mu_{wr_{low}}$)	0.3
Work roll speed ($V_{wr_{up}} = V_{wr_{low}}$)	2, 3, 4 m/s
Entry thickness (h_1)	33, 45, 46, 58 mm
Reduction	20, 27.5, 35 %
Pass line	15, 25, 35, 45 mm
Gravity	9.8 m/sec ²

Figure 9 schematically shows three turn down warping regions during rolling with a pass line for a condition of speed matching. As a result, sub-models to predict the turn down warping in each of the three regions, respectively, were obtained through regression analysis.

Due to the pass line, the mid thickness points of p_4 at the entry side, p_3 at the roll bite, and p_2 and p_1 at the exit side vary continuously during rolling. These variations are the main causes of the asymmetrical deformation along the plate length. Even in the absence of asymmetries due to the differences in size, rotational speed, and frictional conditions between upper and lower rolls, turn down warping can occur in actual plate rolling due to the pass line. As the shape of a typical warping resembles the symmetric ‘bell curve’ shape, regression equations for $\lambda_1 \lambda_2 \lambda_3$ along three different regions were represented by a Gaussian function with a symmetric peak. The general equation for the Gaussian function used in the current study is

$$\lambda_i = g_{\lambda_i} + a_{\lambda_i} \exp \left[-\frac{1}{2} \left(\frac{x - b_{\lambda_i}}{c_{\lambda_i}} \right)^2 \right] \tag{2}$$

where, g_{λ_i} is the intercept, a_{λ_i} is the amplitude, b_{λ_i} is the center, and c_{λ_i} is the width ($c > 0$) of the function.

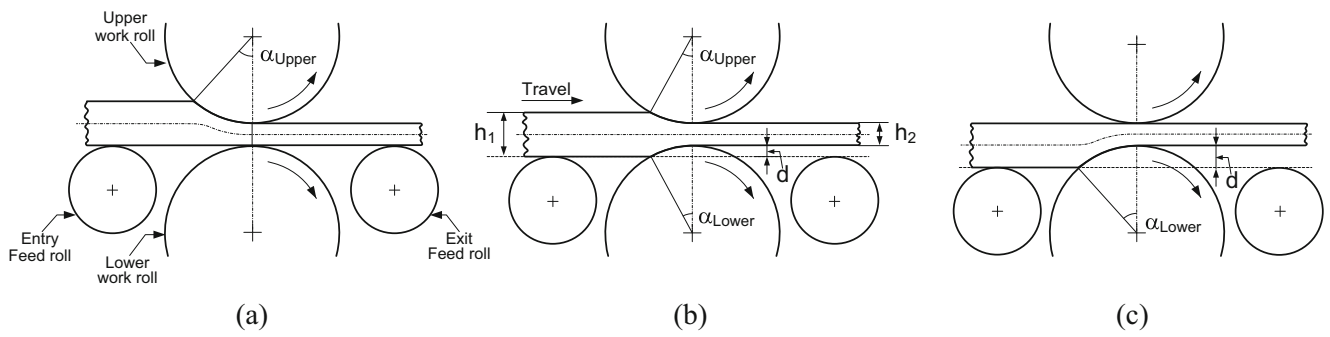


Fig. 8 Three case of pass line use in rolling: **a** Pass line, $d=0$, **b** $d=(h_1-h_2)/2$, **c** $d=(h_1-h_2)$

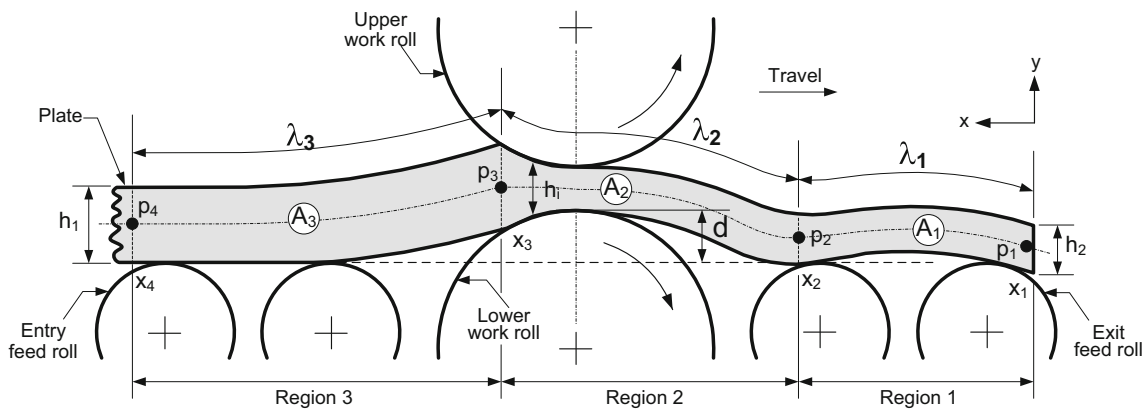


Fig. 9 Classification of three turn down warping regions in rolling with pass line

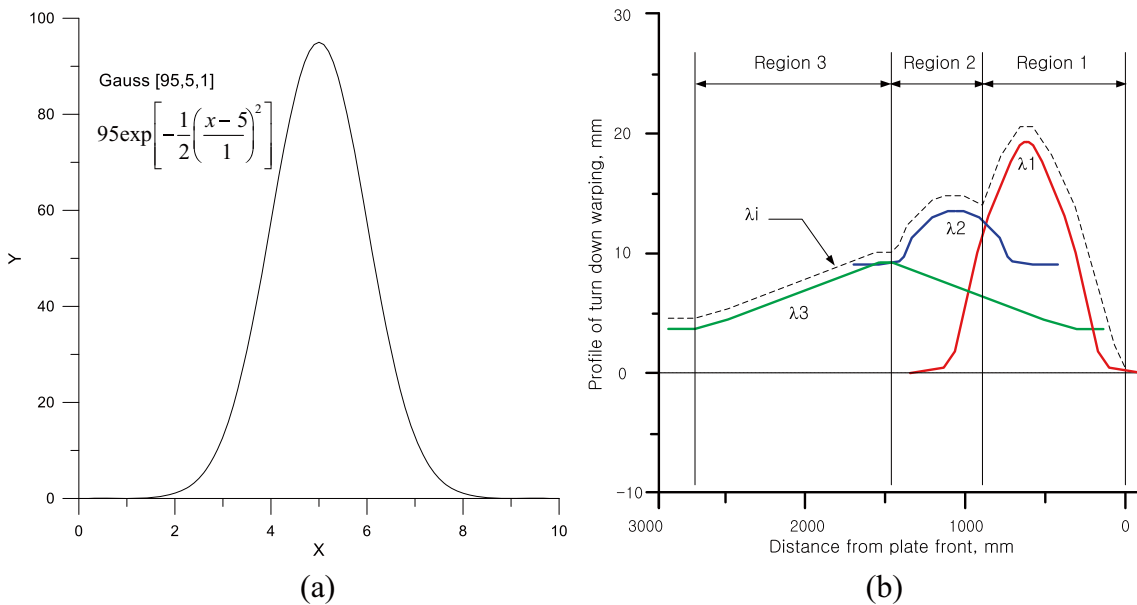


Fig. 10 **a** Gaussian curve fitting; **b** Application of Gaussian curve fitting for turn down warping

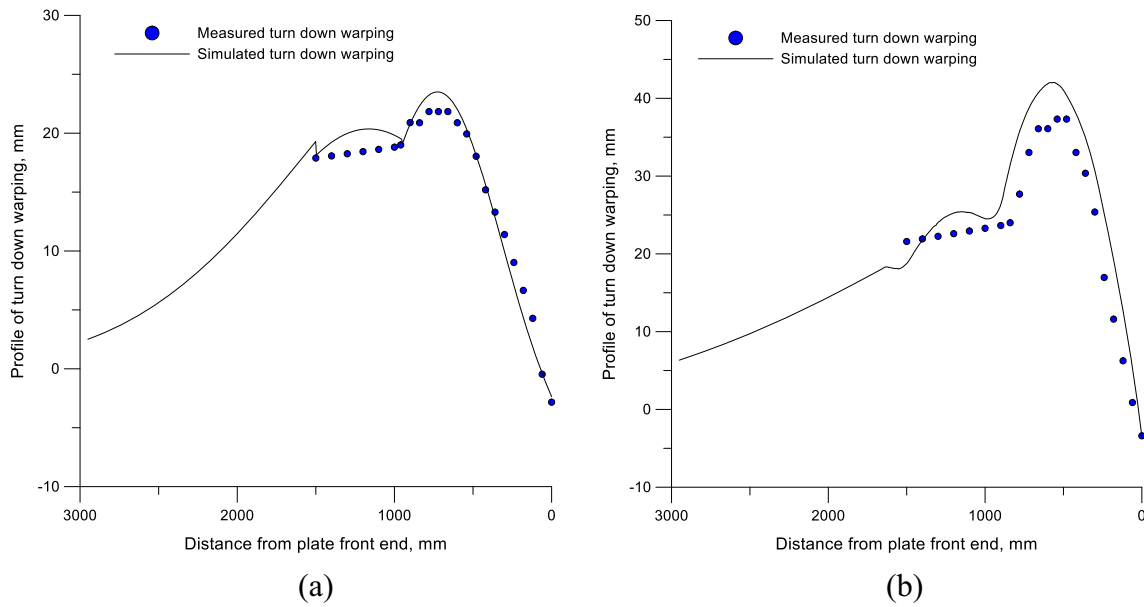


Fig. 11 Comparison of measured and predicted turn down warping: **a** entry thickness 46 mm, reduction 10 %, rolling speed 2.3 m/s, pass line 20 mm; **b** entry thickness 33 mm, reduction 10 %, rolling speed 4.2 m/s, pass line 20 mm

The values for the parameters a_{λ_i} , b_{λ_i} , c_{λ_i} , and g_{λ_i} were obtained by the regressive equation:

$$\begin{aligned} a_{\lambda_i} &= a_0 + a_1 h_1 r + a_2 v d + a_3 v r d \\ b_{\lambda_i} &= b_0 + b_1 h_1 r + b_2 v d + b_3 v r d \\ c_{\lambda_i} &= c_0 + c_1 h_1 r + c_2 v d + c_3 v r d \\ g_{\lambda_i} &= g_0 + g_1 h_1 r + g_2 v d + g_3 v r d \end{aligned} \tag{3}$$

where, h_1 is the entry thickness, r is the reduction, v is the rolling velocity, and d is the pass line.

Figure 10a shows an example of the Gaussian curve fitting for the condition of amplitude 95, center 5, and width 1. Figure 10b shows an actual application of the Gaussian curve fitting for turn down warping. The turn down warping λ_i was determined from the respective profile of the regions λ_1 , λ_2 , and λ_3 .

To check the feasibility of the proposed modeling methodology based on a Gaussian function, turn down image patterns obtained from actual plate rolling data were compared. Figure 11 compares the measured and the predicted turn down

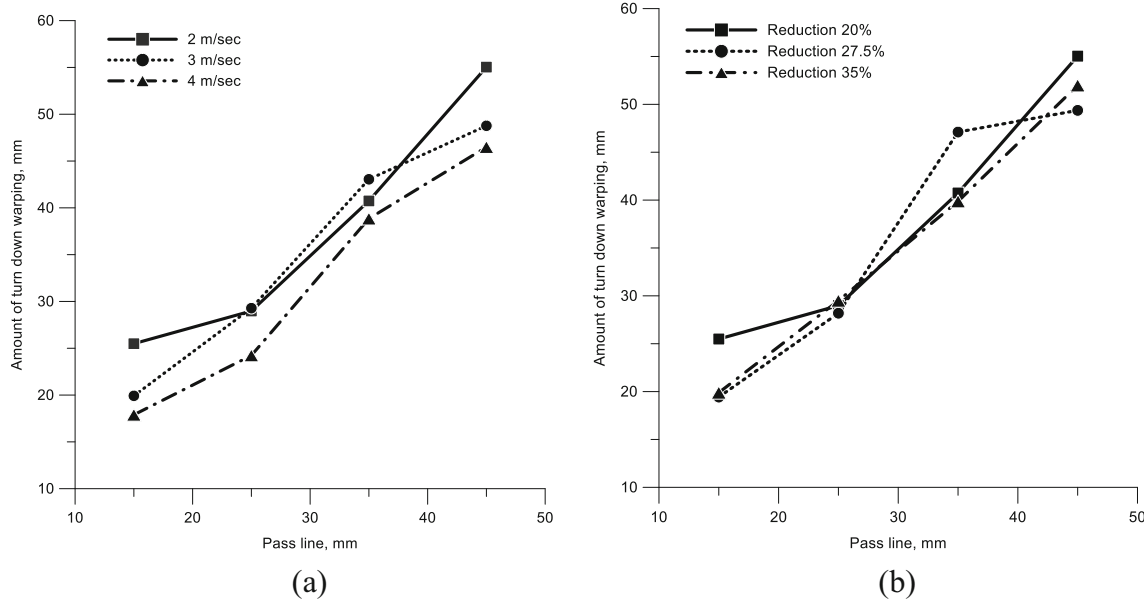


Fig. 12 Simulated results of turn down warping as a function of pass line: **a** effect of rolling speed, **b** effect of reduction

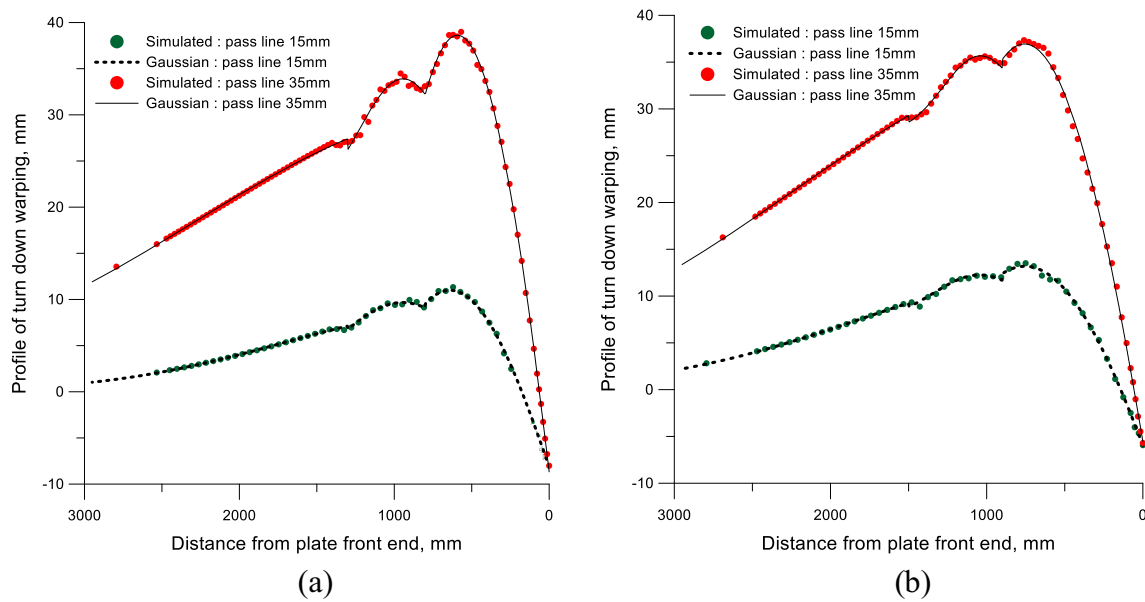


Fig. 13 Comparison of simulated result with prediction model based on Gaussian function: **a** Case 1: entry thickness 58 mm, rolling speed 2 m/s, reduction 27.5 % with a pass line of 15 and 35 mm; **b** Case 2: entry thickness 45 mm, rolling speed 3 m/s, reduction 20 % with a pass line of 15 and 35 mm

Table 2 Coefficients of prediction model based on Gaussian function

Case 1							Case 2						
Pass line	R ²	Length	a	b	c	g	Pass line	R ²	Length	a	b	c	g
15 mm	99 %	λ_1	-46.5	57.5	639.4	710.2	15 mm	99 %	λ_1	-69.2	82.4	755.7	1039.2
	95 %	λ_2	0.2	9.5	947.0	412.5		96 %	λ_2	7.3	5.0	1046.5	295.4
	99 %	λ_3	0.0	8.8	554.4	1160.7		99 %	λ_3	0.0	12.6	452.6	1345.2
35 mm	99 %	λ_1	-199.0	237.6	529.0	888.6	35 mm	99 %	λ_1	-179.9	216.8	757.6	1147.4
	98 %	λ_2	19.7	14.2	943.8	284.9		98 %	λ_2	27.3	8.4	1039.8	238.6
	99 %	λ_3	-0.1	30.5	486.5	1806.5		99 %	λ_3	-0.1	35.3	383.8	1851.4

warpings at a speed match condition for two different sets of process variables. In the case of Fig. 11a, the average deviation and standard deviation are 4.3 and 0.6 mm, respectively, and 1.2 and 0.14 mm for Fig. 11b. In both cases shown in Fig. 11, the predicted patterns agree well with actual patterns, even though the amounts of simulated turn down warping were slightly larger than the actually measured patterns.

Prediction of turn down warping

By using the prediction model, the turn down warping for a condition of speed matching was obtained under various process conditions. Figure 12 shows variations of turn down warping with the pass line. Turn down warping increases with increasing pass line for a given process condition. Turn down warping

Table 3 Coefficients (a_0 - a_3 , b_0 - b_3 , c_0 - c_3 , g_0 - g_3) for the regression equation

	a_0	a_1	a_2	a_3	b_0	b_1	b_2	b_3	c_0	c_1	c_2	c_3	g_0	g_1	g_2	g_3
λ_1	61.9	-1.76	-11.4	0.45	73.1	-2.1	-13.6	0.51	971	-20.7	-1.9	0.43	1268	-40	-12.3	0.7
λ_2	-2.8	-0.68	1.73	0.01	-5.7	0.78	0.34	0.01	1175	-14.1	-0.4	0.30	291	10.3	-7.8	0.67
λ_3	0.06	-0.0006	-0.0074	0.0029	-1.22	-0.31	1.87	0.01	38.5	13.6	-5.91	0.042	919	-7.5	49.7	1.61

increases with decreasing rolling speed—but is not significantly influenced by reduction. The amount of turn down warping for a 45 mm pass line is approximately 2.5 times larger than that of a 15 mm pass line. This result implies that the amount of turn down warping can be decreased by a reduction in the pass line. As shown in Fig. 7, symmetrical rolling is most common in production, so an intentional reduction of pass lines may cause other problems in the rolling operation. As the pass line is the most influential factor on turn down warping, the precise prediction of turn down warping with pass line is essential.

Figure 13 shows the agreement of the regression model based on a Gaussian function with simulated results. As shown in the figure, good agreement can be achieved by using the Gaussian function base model. Table 2 summarizes the coefficients for the regression model shown in Eq. (2). These coefficients are obtained from the regression of FE results. For Fig. 13a, the average and standard deviations for the 15 mm pass line are 0.000032 and 0.13 mm respectively, and 0.000059 and 0.24 mm for the 35 mm pass line. In the case of Fig. 13b, the average and standard deviations for the 15 mm pass line are 0.000043 and 0.18 mm respectively, and are 0.000062 and 0.34 mm for the 35 mm pass line. Table 3 shows the coefficients for the regression model shown in Eq. (3).

From the results shown in Fig. 12, turn down warping at a speed match condition can be successfully predicted by a model and the proposed methodology should be both feasible and reliable for predicting turn down warping.

Conclusions

A prediction model based on a Gaussian function was investigated to estimate turn down warping, and the following conclusions were obtained.

- 1) Even in the absence of asymmetries due to the differences in size, rotational speed, and frictional conditions between the upper roll and the lower roll, turn down warping can occur during actual plate rolling due to the pass line. The amount of turn down warping increases with increases in the pass line for a given rolling condition.
- 2) A model based on a Gaussian function is proposed to predict turn down warping of the plate front end as a function of plate thickness, reduction, rolling speed, and pass line. Coefficients for the model equation obtained from regression analysis of the FE simulation results are reliable for predicting turn down warping.
- 3) The predicted turn down pattern based on a Gaussian function agrees well with measured patterns for industrial rolling. This agreement confirms that the proposed modeling methodology based on a Gaussian function is both feasible and reliable for predicting turn down warping during hot plate rolling.

Acknowledgments This research was partially supported by the program on Fusion Core Technology for Industry (No. 10044681) funded by Ministry of Knowledge Economy (MKE).

References

1. Shivpuri R, Chou PC, Lau CW (1988) Finite element investigation of curling in non-symmetry rolling of flat stock. *Int J Mech Sci* 30: 625–635
2. Yoshii M, Ohmori K, Seto T, Nikaido H, Nishizaki H, Inoue M (1991) Analysis of warping phenomenon in plate rolling. *ISIJ Int* 31:73–978
3. Richelsen AB (1994) Numerical analysis of asymmetrical rolling accounting for difference in friction. *J Mater Process Technol* 45: 149–154
4. Jeswiet J, Greene PG (1998) Experimental measurement of curl in rolling. *J Mater Process Technol* 84:202–209
5. Knight CW, Hardy SJ, Lees AW, Brown KJ (2005) Influence of roll speed mismatch on strip curvature during the roughing stages of a hot rolling mill. *J Mater Process Technol* 168:184–188
6. Farhat-Nia F, Salimi M, Movahhedy MR (2006) Elasto-plastic finite element analytical plate rolling using an ALE approach. *J Mater Process Technol* 177:525–529
7. Gudur PP, Salunkhe MA, Dixit US (2008) A theoretical study on the application of asymmetric rolling for the estimation of friction. *Int J Mech Sci* 50:315–327
8. Anders D, Munker T, Artel J, Weinberg K (2012) A dimensional analysis of front-end bending in plate rolling applications. *J Mater Process Technol* 212:1387–1398
9. Philipp M, Schwenzfeier W, Fischer FD, Wödlinger R, Fischer C (2007) Front end bending in plate rolling influenced by circumferential speed mismatch and geometry. *J Mater Process Technol* 184: 224–232
10. Zhang SH, Zhao DW, Gao CR, Wang GD (2012) Analysis of asymmetrical sheet rolling by slab method. *Int J Mech Sci* 65: 168–176
11. Akbari Mousabi SAA, Ebrahimi SM, Madoliat R (2007) Three dimensional numerical analysis of asymmetric rolling. *J Mater Process Technol* 187–188:725–729
12. Kawalek A (2004) Forming of band curvature in asymmetrical rolling process. *J Mater Process Technol* 155–156:2033–2038
13. Markowski J, Dyja H, Knapinski M, Kawalek A (2003) Theoretical analysis of the asymmetric rolling of sheets on leader and finishing stands. *J Mater Process Technol* 138:183–188
14. Salimi M, Sassani F (2002) Modified slab analysis of asymmetrical plate rolling. *Int J Mech Sci* 44:1999–2023
15. Lu JS, Harrer OK, Schwenzfeier W, Fisher FD (2000) Analysis of the bending of the rolling material in asymmetrical sheet rolling. *Int J Mech Sci* 42:49–61
16. Dvorkin EN, Goldschmidt MB, Cavaliere MA, Amenta PM, Marini O, Stroppiana W (1997) 2D finite element parametric studies of the flat-rolling process. *J Mater Process Technol* 68:99–107
17. Dyja H, Korczak P, Pilaczyk JW, Grzybowski J (1994) Theoretical and experimental analysis of plate asymmetric rolling. *J Mater Process Technol* 45:167–172
18. Ji YH, Park JJ (2009) Development of severe plastic deformation by various asymmetric rolling process. *Mater Sci Eng A* 499:14–17
19. Jin H, Lloyd DJ (2005) The reduction of planar anisotropy by texture modification through asymmetric rolling and annealing in AA5754. *Mater Sci Eng A* 399:358–367
20. Lee SH, Lee DN (2001) Analysis of deformation textures of asymmetrically rolled steel sheets. *Int J Mech Sci* 43:1997–2015

21. Watanabe H, Mukai T, Ishikawa K (2004) Differential speed rolling of an AZ31 magnesium alloy and the resulting mechanical properties. *J Mater Sci* 39:1477–1480
22. Ji YH, Park JJ, Kim WJ (2007) Finite element analysis of severe deformation in Mg–3Al–1Zn sheets through differential-speed rolling with a high speed ratio. *Mater Sci Eng A* 454–455:570–574